



First-in-Human Stage III/IV Melanoma Clinical Trial of Immune Priming Agent IFx-Hu2.0

Joseph Markowitz^{1,7}, Michael Shablott², Andrew S. Brohl^{1,3,7}, Amod A. Sarnaik^{1,7}, Zeynep Eroglu^{1,7}, Nikhil I. Khushalani^{1,7}, Christopher W. Dukes⁶, Alejandra Chamizo¹, Marina Bastawrous², Edward T. Garcia², Ashraf Dehlawi², Pei-Ling Chen^{4,7}, Deanryan B. De Aquino¹, Vernon K. Sondak^{1,7}, Ahmad A. Tarhini^{1,7}, Youngchul Kim⁵, Patricia Lawman², and Shari Pilon-Thomas^{6,7}

ABSTRACT

IFx-Hu2.0 was designed to encode part of the Emm55 protein contained within a plasmid in a formulation intended for transfection into mammalian cells. IFx-Hu2.0 promotes both adaptive and innate immune responses in animal studies. Furthermore, previous studies have demonstrated safety/efficacy in equine, canine, and murine species. We present the first-in-human study of IFx-Hu2.0, administered by intralesional injection into melanoma tumors of seven patients with stage III/IV unresectable melanoma. No dose-limiting toxicities attributable to IFx-Hu2.0 were observed. Grade 1/2

injection site reactions were observed in five of seven patients. IgG and IgM responses to Emm55 peptides and known melanoma antigens were seen in the peripheral blood, suggesting that IFx-Hu2.0 acts as an individualized “in situ vaccine.” Three of four patients previously refractory to anti-PD1 experienced clinical benefit upon subsequent anti-PD1-based treatment. Therefore, this approach is feasible, and clinical/correlative outcomes warrant further investigation for treating patients with metastatic melanoma with an immune priming agent.

Introduction

In 2023, 97,610 cases of invasive melanoma, with 7,990 deaths, were predicted in the United States (1). The response rate of single-agent anti-PD1 (nivolumab and pembrolizumab) is approximately 40%, and in combination with anti-CTLA4 or anti-LAG3 therapy, response rates increase to 50% to 60%, at the cost of significantly increased toxicity (2–8). Talmogene laherparepvec (TVEC) is an oncolytic live virus approved for intralesional administration into cutaneous, in-transit, or nodal melanoma metastases (9). TVEC suffers from many limitations, and there remains a major unmet need for new intralesional immunotherapeutic approaches (10). The properties of IFx-Hu2.0 may allow for an injection schema that circumvents the issue that TVEC needs to be injected every 2 weeks. The intralesional approach is beneficial in melanoma due to readily accessible lesions and minimal systemic toxicity (11).

IFx-Hu2.0 is a plasmid DNA, pAc/emm55, formulated with *in vivo*-jetPEI, a cationic polymer that aids in the cellular uptake of DNA to express the Emm55 protein. It is administered by intralesional injection. Emm55 is a serotyping M-like protein generally expressed on the surface of the bacterium *Streptococcus pyogenes* and is highly antigenic (12, 13). Therefore, it was hypothesized that the Emm55 protein fragment expressed by the IFx-Hu2.0 product acts as an immunologic priming antigen to attract the patient's immune system to tumor cells.

IFx-Hu2.0 injection in a murine B16 melanoma model decreased tumor growth and increased T-cell infiltration. The antigen-specific reactions depended on a Toll-like receptor mechanism (14). Efficacy was also seen in equine melanoma, this time with an IgG response (15). Safety data were available in three species (murine, canine, and equine; ref. 12, 14, 15). Given the preclinical tolerability and effectiveness, we undertook the first-in-human trial to investigate the feasibility of injecting IFx-Hu2.0 intratumorally in patients with unresectable stage III/IV cutaneous melanoma refractory to standard-of-care treatment. The intent was to provide one to two doses of IFx-Hu2.0, and the protocol allowed for posttrial observation on additional melanoma therapies. Herein, we describe the feasibility of utilizing IFx-Hu2.0 and preliminary data suggesting beneficial effects in anti-PD1 refractory patients.

Materials and Methods

Patients were consented to MCC19500 (NCT03655756) using an institutional review board-approved protocol, and patient's informed consent was obtained under the supervision of the Institutional Biosafety Committee. This study was conducted in accordance with the Declaration of Helsinki. To test safety, tolerability, and feasibility, IFx-Hu2.0 was injected (0.1 mg) into cutaneous lesions of adult melanoma patients (ages ≥ 18 years) with unresectable stage III/IV cutaneous melanoma. At least two injectable

¹Department of Cutaneous Oncology, H. Lee Moffitt Cancer Center and Research Institute, Tampa, Florida. ²Morphogenesis, Inc, Tampa, Florida. ³Department of Sarcoma Oncology, H. Lee Moffitt Cancer Center and Research Institute, Tampa, Florida. ⁴Department of Pathology, H. Lee Moffitt Cancer Center and Research Institute, Tampa, Florida. ⁵Department of Biostatistics and Bioinformatics, H. Lee Moffitt Cancer Center and Research Institute, Tampa, Florida. ⁶Department of Immunology, H. Lee Moffitt Cancer Center and Research Institute, Tampa, Florida. ⁷Department of Oncologic Sciences, University of South Florida Morsani School of Medicine, Tampa, Florida.

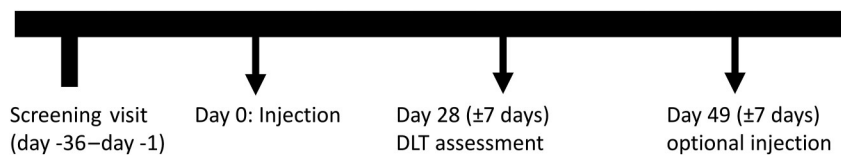
Corresponding Author: Joseph Markowitz, Department of Cutaneous Oncology, H. Lee Moffitt Cancer Center and Research Institute, 10920 McKinley Drive, Tampa, FL 33612. E-mail: joseph.markowitz@moffitt.org

Mol Cancer Ther 2024;23:1139–43

doi: 10.1158/1535-7163.MCT-23-0652

This open access article is distributed under the Creative Commons Attribution-NonCommercial-NoDerivatives 4.0 International (CC BY-NC-ND 4.0) license.

©2024 The Authors; Published by the American Association for Cancer Research

**Figure 1.**

Trial schema. The endpoint was the DLT at 28 days, and if the patient received one dose of IFx-Hu2.0, this was the final study visit. Patients were allowed additional subsequent doses of IFx-Hu2.0 every 3 weeks. One patient received an IFx-Hu2.0 injection at 49 days and then had the final study visit 21 days later.

lesions ≥ 3 mm in size were required for entry into the study. Subjects were all evaluated for anti-PD1 therapy, TVEC, and/or V-Raf Murine Sarcoma Viral Oncogene Homolog B (BRAF) inhibition as indicated in the FDA labels for those agents and were deemed not candidates if they were refractory to approved therapies or unable (due to immune-based diseases)/unwilling to tolerate the adverse effects of these agents. Small brain metastases (≤ 1 cm) were permitted, assuming a longer than 3-month life expectancy and any received concurrent radiation was at a site distant from the intralésional injection site. Subjects could not receive any other concurrent anticancer therapies, nor could they have uncontrolled hepatitis/HIV infection, organ transplantation, or immunosuppression requiring more than 10 mg prednisone-equivalent daily. Trial subjects had the option of continued dosing every 3 weeks if they tolerated the first dose and showed no evidence of progression. The study's success was defined as treating five of six subjects without dose-limiting toxicity (DLT) at 28 days. Once treatment with IFx-Hu2.0 ended, subjects were permitted to receive any subsequent therapy at the discretion of their treating physician, and responses to the next line of therapy were monitored clinically and recorded (Fig. 1).

Biopsies were taken before and after treatment, snap-frozen, and/or placed in formalin for formalin-fixed, paraffin-embedded processing. In addition, plasma samples were collected before the first dose and during the 4-week DLT period. Plasma was separated from peripheral blood samples as previously described (16).

Frozen tissue analysis

mRNA was extracted from frozen tissue specimens using the RNeasy UCP Micro Kit and shipped to NanoString for analysis using the PanCancer IO 360 expression panel (17). At the same time points of tissue collection, paired plasma samples were collected.

Plasma analyses

Plasma samples were screened on Olink Inflammation (v.3022) and Immunooncology (v.3111) panels to measure cytokines and chemokines in plasma as per the manufacturer's instructions (18, 19). Plasma samples were also subjected to melanoma-associated antigen-antibody IgG and IgM response profiling. Pre- and post-treatment plasma samples from subjects were diluted 1:100. Samples from subject M10106 were diluted 1:250. Diluted samples were screened on PEPperPRINT PEPperCHIP Melanoma Antigen Microarray for 21 melanoma antigens as per the manufacturer's instructions (18, 19). Hemagglutinin, GS linker, and polio control peptides were included on the chip as a series of 15 amino acid peptides. Subject antibody binding was detected using goat anti-human IgG (Fc) DyLight680 (0.1 $\mu\text{g}/\text{mL}$) and goat anti-human IgM (μ chain) DyLight800 (0.2 $\mu\text{g}/\text{mL}$) and imaged on a LI-COR Odyssey Imaging System. In addition, the PEPperPRINT technology was used to analyze the Emm55-specific IgG and IgM antibody

responses. The Emm55 amino acid sequence was converted into 15 amino acid peptides with an overlap of 14 amino acids. The neutral linkers were printed in duplicate on a custom PEPperPRINT PEPperCHIP, which also contained hemagglutinin and polio control peptides. Pre- and posttreatment plasma samples were screened at a dilution of 1:150. Staining was identical to the above except that an Innopsys InnoScan 710-IR microarray scanner was used to image the slides.

Statistical analyses

Differential expression analysis of NanoString mRNA data was performed using the DESeq2 method (20). A volcano plot was constructed to depict a \log_2 -fold change in mRNA expression levels measured in the patient's tissue pre- versus post-therapy and a P -value derived from the DESeq2 method. Significant genes (\log_2 -fold, P -value < 0.05) were analyzed via core analysis in Ingenuity pathway analysis and visualized within the graphical summary tab. Box plots were also constructed to analyze trends for individual mRNA in IFx-Hu2.0-injected versus uninjected lesions. To identify differentially abundant proteins between pre- and posttreatment samples for each patient, an outlier linear regression analysis test was performed for each Olink Inflammation and Immunooncology panel data (21). In brief, studentized residuals, i.e., the scaled distance between the observed value and predicted value, were calculated, and proteins with absolute studentized residuals > 1.97 were identified to have differential abundance. Similar analyses were performed to measure IgG and IgM on the PEPperPRINT melanoma chip. In addition, the appearance or disappearance of recognition of melanoma antigens in plasma was depicted via a heatmap graph.

Data availability

The data generated in this study are available upon request from the corresponding author.

Results

Clinical results

Eight subjects were screened (M10101–8). One subject failed screening (M10102), whereas seven met the eligibility requirements for the trial. Subjects ranged in age from 60 to 85 years. The primary endpoint was met in that six patients who completed the DLT period experienced no DLT related to IFx-Hu2.0. Only grade 1 and 2 toxicities deemed related to IFx-Hu2.0 were encountered. These were expected for intralésional injection (i.e., injection site reactions) and managed with conservative measures. In brief, in the seven patients, observed toxicities included grade 1 to 2 injection site reactions in five patients, grade 1 bleeding in one patient, grade 1 to 2 pain in two patients, grade 1 lymphopenia in one patient, and grade 1 pruritis in one patient. No grade 3 or greater toxicities related to the study drug were observed. One grade 5 toxicity (death due to *Clostridium septicum* infection 20 days post injection at a site

Table 1. Adverse events related to IFx-Hu2.0 are G1–2.

| Adverse event preferred term | Overall related counts | |
|------------------------------|------------------------|---------|
| | Grade 1 | Grade 2 |
| Total (n = 7) | | |
| Back pain | 1 | 0 |
| Injection site reaction | | |
| Erythema | 4 | 0 |
| Erythema w/pruritis | 0 | 1 |
| Erythema/pain | 1 | 0 |
| Pruritus | 1 | 0 |
| Site reaction | 1 | 0 |
| Tumor hemorrhage | 2 | 0 |
| Tumor pain | 0 | 2 |
| Hypoesthesia | 1 | 0 |
| Lymphocyte count decreased | 1 | 0 |
| Pruritus | 1 | 0 |
| Tumor hemorrhage | 1 | 0 |

distant from study drug injection sites) was deemed unlikely related to the study drug after a thorough investigation, including autopsy illustrating likely left groin source of infection (Table 1; Supplementary Table S1). Six patients had injections at one time point, and one patient had injections at two time points (Supplementary Table S2). Three patients had stable disease, and three patients progressed by RECIST 1.1 at the 30-day follow-up visit. Lactate dehydrogenase values were within normal limits for all evaluable patients pre-/post-therapy, and there were no significant differences in neutrophil/lymphocyte ratios.

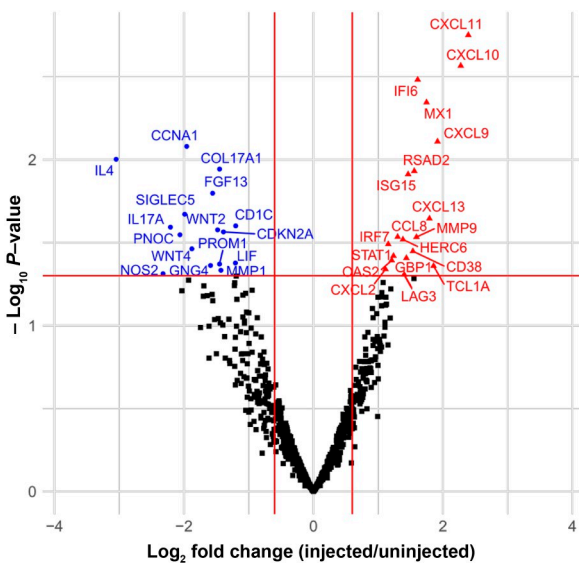


Figure 2. Volcano gene plot increased and decreased expression in specimens in which paired uninjected prior to therapy and injected lesions were available for analysis (M10104, M10107, and M10108). The volcano plot illustrates the importance of these genes in interferon responses and antigen-dependent responses.

Post-protocol therapy responses

Of the seven patients, six received further anticancer treatment after coming off protocol. Three of four anti-PD1 refractory patients had evidence of clinical benefit after post-protocol retreatment with anti-PD1-based therapy [stable disease lasting >2 years followed by surgical resection with progression-free survival (PFS) post-protocol therapy (PFS2) >3.66 years; PFS2 of 1.08 years; and partial response (PR) subsequently surgically resected and rendered no evidence of disease—PFS2 of 1.66 years]. PFS2 on subsequent anti-PD1 therapy is depicted in Supplementary Table S2 and demonstrates increased PFS2 compared with that of historical controls after anti-PD1 failure.

Effects of IFx-Hu2.0 on promoting immune responses

Paired samples from each patient collected before and approximately 30 days after injection were analyzed using the mRNA panel. Multiple genes associated with B-cell antibody-dependent immune responses, including CXCL13 and CD38, were upregulated ($P < 0.05$) in lesions biopsied post-therapy on protocol, in addition to immune checkpoint molecules such as LAG3 and proteins indicative of a strong interferon response (STAT1, STAT2, and multiple IRFs). Both innate and adaptive immune responses were detected in the injected lesions (Fig. 2; Supplementary Fig. S1). Genes associated with anti-PD1 or LAG3 response, such as CXCL11, CXCL13, IFI6, MX1, and LAG3, were upregulated ($P < 0.05$). In addition, several oncogenes were downregulated (*WNT2*, *WNT4*, and *PNO*C). A strong interferon response was noted along with processes involved in antigen presentation and antiviral responses.

Given these findings, we measured the cytokines as well as melanoma- and Emm55-specific peptide antigens in the plasma. Cytokine/chemokine analysis demonstrated a variable response in patient-derived plasma samples, suggesting that an individualized immune response is generated by IFx-Hu2.0 activity (Supplementary Figs. S2 and S3). Although all patients had increased antibody production against melanoma-specific peptides (Fig. 3; Supplementary Figs. S4–S7), the combination of peptides recognized by each patient was unique. In each patient, IgG and IgM reactivity to overlapping Emm55 peptides (5–14 amino acid residues) was also detected, but the peptides recognized were unique for each patient. The antibody responses to Emm55-specific and melanoma-specific peptides increased after therapy. In many cases, antibody responses were present after treatment, whereas none existed before therapy, as depicted via heatmap analysis (Fig. 3; Supplementary Figs. S6 and S7). IgG and IgM responses to individual peptides differed for different patients.

Discussion

Melanoma cells may “hide” tumor-specific antigens from the immune system or take advantage of the normal inhibitory immune pathways designed to protect a person from autoimmunity (22). M-cell surface proteins encoded by *emm* genes act as antiphagocytic factors, crucial for defense against innate human immunity (23). We utilized a fragment of an M protein to generate an immune response expressed in melanoma tumors via a plasmid approach such that the body recognizes the tumor as foreign. Due to high variability at the N-terminal region of M proteins, more than 200 distinct types have been recorded in public databases. M proteins have been considered vaccine candidates against group A *Streptococcus*-mediated strep throat infection and suppurative skin diseases (24). However, some M proteins bind collagen and may cause side effects such as acute rheumatic fever in humans through molecular mimicry of collagen (25). Emm55 has been shown not to bind collagen because of the

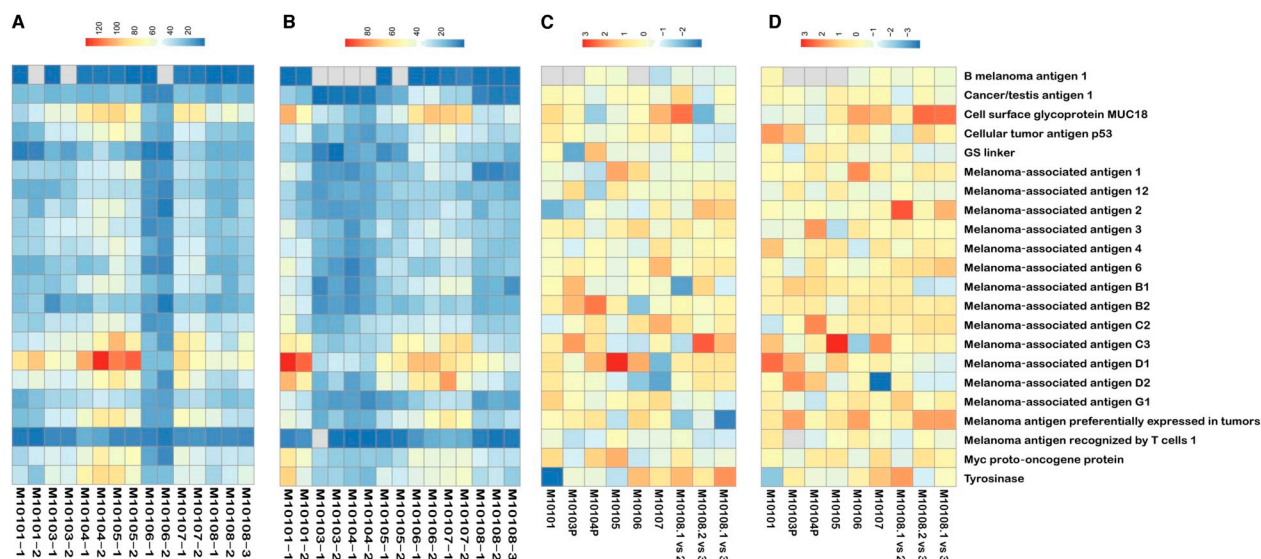


Figure 3.

A, Melanoma-specific peptides in the plasma responsible for IgM responses present after therapy and absent before therapy. We have labeled the samples by patient number and the time point Z (M1010X-Y), where 1 = pretreatment, 2 = DLT visit, 3 = 3 weeks after the second injection. **B,** Melanoma-specific peptides responsible for IgG responses present after therapy and absent before therapy. **C,** Changes in recognition of melanoma-specific peptides after injection of IFX-Hu2.0 responsible for IgM responses. **D,** Changes in recognition of melanoma-specific peptides after injection of IFX-Hu2.0 responsible for IgG responses. The scales in each heatmap represent the number of peptides detected.

conformational influences of flanking sequences (26). No rheumatological clinical effects were seen in this trial. Systemic immune responses elicited by IFX-Hu2.0 in B16-bearing mice are antigen-specific, and equine melanoma responses are IgG-specific (14, 15). Surface expression of the Emm55 antigen through intralesional injection of pAc/emm55 (Supplementary Fig. S8) is proposed to engage the patient's immune system to thwart the tumor's ability to evade surveillance by exposing multiple patient-specific tumor antigens and activating an effective immune response.

With intralesional injection, different tumor-related antigens can be recognized in individual patients, offering a personalized "in situ vaccine" approach. In this trial, IFX-Hu2.0 was shown to be safe to inject into melanoma lesions, and there were no DLTs attributable to IFX-Hu2.0. The data from clinical trial specimens suggest that IFX-Hu2.0 acting through the interferon response and Toll-like receptors (Fig. 1) can be an active bridge between the innate and adaptive immune responses by activating interferon pathways and promoting antigen recognition of Emm55 peptides. There are IgG and IgM antigen-specific responses to both the Emm55 protein- and melanoma-specific antigens in patient-derived plasma. Posttreatment evidence of clinical benefit for retreatment with anti-PD1 antibodies in three patients previously refractory to those agents is encouraging and suggests the possibility of synergy if IFX-Hu2.0 is administered in conjunction with immunotherapy. Given that response to anti-PD1 depends on antibody- and interferon-dependent responses (27, 28), further development of this agent in melanoma is warranted.

Authors' Disclosures

J. Markowitz reports grants from Bankhead Coley, NIH, and Morphogenesis, Inc. during the conduct of the study; grants from Ocala Dames Foundation and Microba

and other support from Merck outside the submitted work; and a patent for Provisional Patent pending to Moffitt Cancer Center. M. Shablott reports personal fees and other support from Morphogenesis/TuHURA Biosciences outside the submitted work. A.S. Brohl reports personal fees from Bayer and Deciphera outside the submitted work. A.A. Sarnaik reports grants and personal fees from Iovance Biotherapeutics, and personal fees from Guidepoint, Defined Health, Boxer Capital, Huron Consulting Group, KeyQuest Health, Istari, Market Access, and Gerson Lehrman Group outside the submitted work; and a patent for US14/974,357 issued. Z. Eroglu reports grants and personal fees from Pfizer; personal fees from Regeneron, Incyte, Eisai, Sun Pharma, and Genentech; and grants from Novartis and Boehringer Ingelheim outside the submitted work. N.I. Khushalani reports grants from Morphogenesis, Inc. during the conduct of the study; grants from Bristol Myers Squibb, GlaxoSmithKline, HUYABIO International, Celgene, and Modulation Therapeutics; grants, personal fees, and other support from Regeneron; grants and personal fees from Merck, Novartis, and Replimune; personal fees from Iovance Biotherapeutics, Nektar, and Instil Bio; personal fees and other support from Castle Biosciences; personal fees from Incyte and AstraZeneca; and other support from Asensus Surgical, Bellicum Pharmaceuticals, and Amarin outside the submitted work. M. Bastawrous reports a patent for US20200000901A1 issued. V.K. Sondak reports personal fees from Merck, BMS, Alkermes, Regeneron, and Iovance Biotherapeutics and other support from SkylineDx outside the submitted work. A.A. Tarhini reports grants from Regeneron, Genentech-Roche, Bristol Myers Squibb, Sanofi-Genzyme, Iovance Biotherapeutics, Merck, Pfizer, OncoSec, Scholar Rock, InflaRx GmbH, Agenus, and Acrotech, and personal fees from Bristol Myers Squibb, Merck, Regeneron, Sanofi-Genzyme, Partner Therapeutics, ConcertAI, AstraZeneca, Genentech-Roche, and Pfizer outside the submitted work. P. Lawman reports association with a commercial company. S. Pilon-Thomas reports grants from Morphogenesis, Inc. and Bankhead-Coley during the conduct of the study; personal fees from Morphogenesis, Seagen, Inc., and KSQ Therapeutics, Inc., grants from Turnstone Biologics, Proectus Biopharmaceuticals, Intellia Therapeutics, and Dyve Biosciences, and grants and other support from Iovance Biotherapeutics outside the submitted work; and a patent for Intellectual Property pending and licensed to TuHURA Biopharma. No disclosures were reported by the other authors.

Authors' Contributions

J. Markowitz: Conceptualization, resources, data curation, formal analysis, supervision, funding acquisition, investigation, visualization,

methodology, writing–original draft, project administration, writing–review and editing. **M. Shablott:** Data curation, formal analysis, investigation, methodology, writing–original draft, writing–review and editing. **A.S. Brohl:** Investigation, writing–review and editing. **A.A. Sarnaik:** Investigation, writing–review and editing. **Z. Eroglu:** Investigation, writing–review and editing. **N.I. Khushalani:** Investigation, writing–review and editing. **C.W. Dukes:** Formal analysis, visualization, writing–original draft, writing–review and editing. **A. Chamizo:** Data curation, formal analysis, visualization, writing–original draft. **M. Bastawrous:** Investigation, writing–review and editing. **E.T. Garcia:** Investigation, writing–review and editing. **A. Delhawi:** Writing–review and editing. **P.-L. Chen:** Investigation, visualization, writing–review and editing. **D.B. De Aquino:** Data curation, investigation, writing–review and editing. **V.K. Sondak:** Investigation, writing–review and editing. **A.A. Tarhini:** Investigation, writing–review and editing. **Y. Kim:** Formal analysis, supervision, investigation, writing–original draft, writing–review and editing. **P. Lawman:** Conceptualization, investigation, writing–original draft, writing–review and editing. **S. Pilon-**

Thomas: Conceptualization, supervision, writing–original draft, writing–review and editing.

Acknowledgments

This research was conducted in part by Biostatistics & Bioinformatics Shared Resource and Collaborative Data Services Core at the H. Lee Moffitt Cancer Center & Research Institute, a comprehensive cancer center designated by the NCI (P30-CA076292) and funded in part by KO8CA252164 (J. Markowitz), Bankhead Coley Grant (J. Markowitz), and Morphogenesis (Moffitt Cancer Center).

Note

Supplementary data for this article are available at Molecular Cancer Therapeutics Online (<http://mct.aacrjournals.org/>).

Received September 21, 2023; revised January 21, 2024; accepted April 17, 2024; published first April 24, 2024.

References

- Siegel RL, Miller KD, Wagle NS, Jemal A. Cancer statistics, 2023. *CA Cancer J Clin* 2023;73:17–48.
- Moreno BH, Parisi G, Robert L, Ribas A. Anti-PD-1 therapy in melanoma. *Semin Oncol* 2015;42:466–73.
- Jarboe J, Gupta A, Saif MW. Therapeutic human monoclonal antibodies against cancer. *Methods Mol Biol* 2014;1060:61–77.
- Pennock GK, Chow LQ. The evolving role of immune checkpoint inhibitors in cancer treatment. *Oncologist* 2015;20:812–22.
- Weber JS, D'Angelo SP, Minor D, Hodi FS, Gutzmer R, Neyns B, et al. Nivolumab versus chemotherapy in patients with advanced melanoma who progressed after anti-CTLA-4 treatment (CheckMate 037): a randomised, controlled, open-label, phase 3 trial. *Lancet Oncol* 2015;16:375–84.
- Lesokhin AM, Callahan MK, Postow MA, Wolchok JD. On being less tolerant: enhanced cancer immunosurveillance enabled by targeting checkpoints and agonists of T cell activation. *Sci Transl Med* 2015;7:280sr1.
- Postow MA, Callahan MK, Wolchok JD. Immune checkpoint blockade in cancer therapy. *J Clin Oncol* 2015;33:1974–82.
- Tawbi HA, Schadendorf D, Lipson EJ, Ascierto PA, Matamala L, Castillo Gutierrez E, et al. Relatlimab and nivolumab versus nivolumab in untreated advanced melanoma. *N Engl J Med* 2022;386:24–34.
- Kaufman HL, Shalhout SZ, Iodice G. Talimogene laherparepvec: moving from first-in-class to best-in-class. *Front Mol Biosci* 2022;9:834841.
- Carr MJ, Sun J, DePalo D, Rothermel LD, Song Y, Straker RJ, et al. Talimogene laherparepvec (T-VEC) for the treatment of advanced locoregional melanoma after failure of immunotherapy: an international multi-institutional experience. *Ann Surg Oncol* 2022;29:791–801.
- Sloot S, Rashid OM, Sarnaik AA, Zager JS. Developments in intralesional therapy for metastatic melanoma. *Cancer Control* 2016;23:12–20.
- Ramiya VK, Jerald MM, Lawman PD, Lawman MJ. Autologous tumor cells engineered to express bacterial antigens. *Methods Mol Biol* 2014;1139:243–57.
- Glikin GC, Finocchiaro LME. Clinical trials of immunogene therapy for spontaneous tumors in companion animals. *ScientificWorldJournal* 2014;2014: 718520.
- Bunch BL, Kodumudi KN, Scott E, Morse J, Weber AM, Berglund AE, et al. Anti-tumor efficacy of plasmid encoding emm55 in a murine melanoma model. *Cancer Immunol Immunother* 2020;69:2465–76.
- Brown EL, Ramiya VK, Wright CA, Jerald MM, Via AD, Kuppala VN, et al. Treatment of metastatic equine melanoma with a plasmid DNA vaccine encoding *Streptococcus pyogenes* EMM55 protein. *J Equine Vet Sci* 2014;34: 704–8.
- Markowitz J, Abrams Z, Jacob NK, Zhang X, Hassani JN, Latchana N, et al. MicroRNA profiling of patient plasma for clinical trials using bioinformatics and biostatistical approaches. *Oncotargets Ther* 2016;9:5931–41.
- Cesano A. nCounter[®] PanCancer immune profiling panel (NanoString Technologies, Inc., Seattle, WA). *J Immunother Cancer* 2015;3:42.
- Heiss K, Heidepriem J, Fischer N, Weber LK, Dahlke C, Jaenisch T, et al. Rapid response to pandemic threats: immunogenic epitope detection of pandemic pathogens for diagnostics and vaccine development using peptide microarrays. *J Proteome Res* 2020;19:4339–54.
- Stadler V, Felgenhauer T, Beyer M, Fernandez S, Leibe K, Guttler S, et al. Combinatorial synthesis of peptide arrays with a laser printer. *Angew Chem Int Ed Engl* 2008;47:7132–5.
- Love MI, Huber W, Anders S. Moderated estimation of fold change and dispersion for RNA-seq data with DESeq2. *Genome Biol* 2014;15:550.
- Thompson WR. On a criterion for the rejection of observations and the distribution of the ratio of deviation to sample standard deviation. *Ann Math Stat* 1935;6:214–9.
- Chen DS, Mellman I. Oncology meets immunology: the cancer-immunity cycle. *Immunity* 2013;39:1–10.
- Nitsche-Schmitz DP, Rohde M, Chhatwal GS. Invasion mechanisms of gram-positive pathogenic cocci. *Thromb Haemost* 2007;98:488–96.
- Dale JB, Smeesters PR, Courtney HS, Penfound TA, Hohn CM, Smith JC, et al. Structure-based design of broadly protective group A streptococcal M protein-based vaccines. *Vaccine* 2017;35:19–26.
- Dinkla K, Nitsche-Schmitz DP, Barroso V, Reissmann S, Johansson HM, Frick IM, et al. Identification of a streptococcal octapeptide motif involved in acute rheumatic fever. *J Biol Chem* 2007;282:18686–93.
- Reissmann S, Gillen CM, Fulde M, Bergmann R, Nerlich A, Rajkumari R, et al. Region specific and worldwide distribution of collagen-binding M proteins with PARF motifs among human pathogenic streptococcal isolates. *PLoS One* 2012;7:e30122.
- Benci JL, Johnson LR, Choa R, Xu Y, Qiu J, Zhou Z, et al. Opposing functions of interferon coordinate adaptive and innate immune responses to cancer immune checkpoint blockade. *Cell* 2019;178:933–48.e14.
- Helminck BA, Reddy SM, Gao J, Zhang S, Basar R, Thakur R, et al. B cells and tertiary lymphoid structures promote immunotherapy response. *Nature* 2020; 577:549–55.